REVIEWS

Light in tiny holes

C. Genet[1] & T. W. Ebbesen[1]

The presence of tiny holes in an opaque metal film, with sizes smaller than the wavelength of incident light, leads to a wide variety of unexpected optical properties such as strongly enhanced transmission of light through the holes and wavelength filtering. These intriguing effects are now known to be due to the interaction of the light with electronic resonances in the surface of the metal film, and they can be controlled by adjusting the size and geometry of the holes. This knowledge is opening up exciting new opportunities in applications ranging from subwavelength optics and optoelectronics to chemical sensing and biophysics.

A hole in a screen is probably the simplest optical element possible, and was an object of curiosity and technological application long before it was scientifically analysed. A pinhole was at the heart of the camera obscura used by the Flemish painters in the sixteenth century to project an image (albeit upside down) onto their canvases. It was in the middle of the seventeenth century that Grimaldi first described diffraction from a circular aperture[1], contributing to the foundation of classical optics. Despite their apparent simplicity and although they were much larger than the wavelength of light, such apertures remained the object of scientific study and debates for centuries thereafter, as an accurate description and experimental characterization of their optics turned out to be extremely difficult.

In the twentieth century, the interest naturally shifted to subwavelength holes as the technology evolved towards longer wavelengths of the electromagnetic spectrum. With the rising importance of microwave technology in the war effort of the 1940s, Bethe treated the diffractive properties of an idealized subwavelength hole, that is, a hole in a perfectly conducting metal screen of zero thickness[2] (Box 1). His predictions, notably that the optical transmission would be very weak, became the reference for issues associated with the miniaturization of optical elements and the development of modern characterization tools beyond the diffraction limit, such as the scanning near-field optical microscope (SNOM), which typically has a small aperture in the metal-coated tip as the probing element[3].

In this context, the report of the extraordinary transmission phenomenon through arrays of subwavelength holes milled in an opaque metal screen[4] generated considerable interest because it showed that orders of magnitude more light than Bethe's prediction could be transmitted through the holes. This has since stimulated much fundamental research and promoted subwavelength apertures as a core element of new optical devices. Central to this phenomenon is the role of surface waves such as surface plasmons (SP), which are essentially electromagnetic waves trapped at a metallic surface through their interaction with the free electrons of the metal[5,6] (Box 2). This combination of surface waves and subwavelength apertures is what distinguishes the enhanced transmission phenomenon from the idealized Bethe treatment and gives rise to the enhancement. Moreover, modern nanofabrication techniques allow us to tailor the dynamics of this combination by structuring the surface at the subwavelength scale. This opens up a wealth of possibilities and applications from chemical sensors to atom optics.

We will review here the present understanding of the transmission through subwavelength apertures in metal screens, starting for the sake of clarity with simple isolated holes and ending with arrays. As we will see, SPs play an essential role at optical wavelengths in all the considered structures. Applications such as tracking single molecule fluorescence in biology, enhanced vibrational spectroscopy of molecular monolayers and ultrafast photodetectors for optoelectronics illustrate the broad implications for science and technology.

Single apertures

Figure 1a shows a single hole milled in a free-standing Ag film, characterized by both the diameter of the hole and its depth. When Bethe considered such a system, he idealized the structure by assuming that the film was infinitely thin and that the metal was a perfect conductor. With these assumptions, he derived a very simple expression for the transmission efficiency η_B (normalized to the aperture area)[2]:

$$\eta_B = 64(kr)^4/27\pi^2 \quad (1)$$

where $k = 2\pi/\lambda$ is the norm of the wavevector of the incoming light of wavelength λ, and r is the radius of the hole. It is immediately apparent that η_B scales as $(r/\lambda)^4$ and that therefore we would expect the optical transmission to drop rapidly as λ becomes larger than r, as shown in Box 1. In addition, the transmission efficiency is further attenuated exponentially if the real depth of the hole is taken into account[7]. This exponential dependence reflects the fact that the light cannot propagate through the hole if $\lambda > 4r$, whereupon the transmission becomes a tunnelling process. The cutoff condition $\lambda > 4r$ is of course a first approximation and in real situations the cutoff occurs at longer wavelengths when the finite conductivity is taken into account[8] (see Box 1).

Bethe also predicted that the light would diffract as it emerges from the hole in an angular pattern that depends on the orientation relative to the polarization of the incident light[2]. If the diffraction pattern is scanned along the direction of the incoming polarization the intensity should be constant (like a spherical wave in a plane) while in the perpendicular direction, the intensity decreases with increasing angle (the angular dependence is a $\cos^2\theta$ function, typical of a dipole emission pattern).

The increasing use of SNOM and interest in the extraordinary transmission phenomenon have stimulated experimental[9–11] and theoretical[12–16] studies, the results of which challenge Bethe's predictions. In particular, it has become possible to measure the transmission and diffraction from a single subwavelength aperture in a metallic film at optical wavelengths[9–11]. Angular measurements at

[1]ISIS, Université Louis Pasteur and CNRS (UMR7006), 8 allée G. Monge, 67000 Strasbourg, France.

the exit of subwavelength apertures have revealed that the light diffracts less than expected[9,10]. Similarly, the transmitted light can have unexpected features[10]. The simple circular aperture of Fig. 1a has a transmission spectrum with a peak as shown in Fig. 1b not predicted by equation (1) or by other conventional theories[2,7]. Similar measurements can be made on a rectangular hole (Fig. 1c) where the spectrum becomes sensitive to the incident light polarization as can be seen in Fig. 1d. The appearance of such resonant peaks can be understood as the excitation of SP modes at the edges of the hole, a type known as localized SP that has been confirmed by theoretical studies[14]. By aligning the incoming polarization on either the short or long axis of the rectangular hole, we can selectively excite the corresponding localized SPs (Fig. 1d). Such behaviour is very reminiscent of elongated metal particles, the colours of which are also determined by localized SPs. Whereas the localized SP modes are defined by the lateral dimensions of the aperture, theoretical studies have shown that in addition to such SP modes[14] other resonant modes defined along the depth of the hole might also be present and contribute to the transmission signal[12]. Further experimental studies on this issue at optical wavelengths are necessary.

Bethe's theory describes the transmission as a smooth decreasing function of the wavelength, as given by equation (1) and shown in Box 1, whereas the experiments discussed above reveal the presence of a resonance superimposed on a smooth background, thus providing an enhancement at the resonant wavelengths. In all the structures presented in this review, it is always the presence of some type of resonance that leads to transmission enhancement. This reveals yet again that Bethe's theory is too idealized to treat situations where surface modes are involved and where propagating or evanescent modes can additionally be excited inside the hollow aperture[12], thereby significantly underestimating the transmission efficiency. We define the transmission as being extraordinary when it is so enhanced that the transmission efficiency η is larger than 1, in other words when the flux of photons per unit area emerging from the hole is larger than the incident flux per unit area. As we shall see in the next sections, η can be much larger than one for certain aperture structures under appropriate conditions.

For experimental reasons, it is very difficult to quantify η for a single hole. As was pointed out above, the emission pattern from a singe aperture in a real metal is not isotropic and therefore the absolute transmission can only be determined by measuring the absolute intensity over all angles and then summing the data. This remains an experimental challenge. As we shall see in the section on optimizing

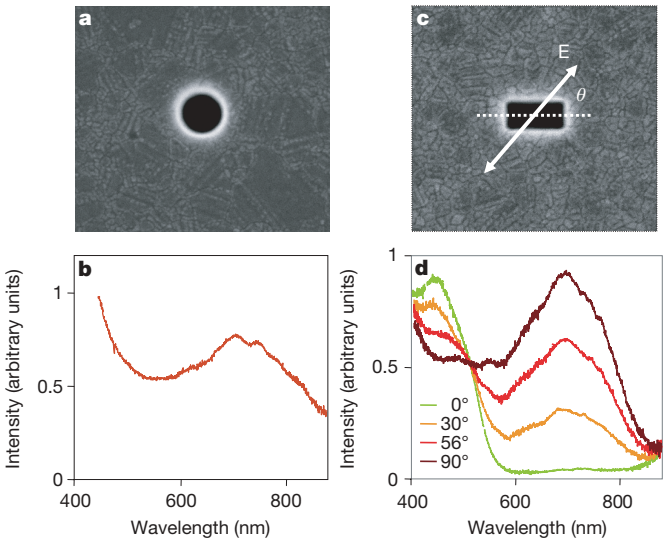

Figure 1 | Optical transmission properties of single holes in metal films. The holes were milled in suspended optically thick Ag films illuminated with white light. **a**, A circular aperture and **b**, its transmission spectrum for a 270 nm diameter in a 200-nm-thick film. **c**, A rectangular aperture and **d**, its transmission spectrum as a function of the polarization angle θ for the following geometrical parameters: 210 nm × 310 nm, film thickness 700 nm. Figure adapted from ref. 10, with permission.

Box 1 | Light transmission through apertures

When light scatters through apertures, it diffracts at the edges. In the subwavelength regime, Bethe was able to give a theoretical description of the diffraction of light at a given wavelength λ through a circular hole of radius $r << \lambda$ in the idealized situation of an infinitely thin and perfect metal sheet. He has shown that the transmission $T(\lambda)$ scales uniformly with the ratio of r to λ to the power of four, as described in equation (1) and schematically shown below in Box 1 Fig. 1.

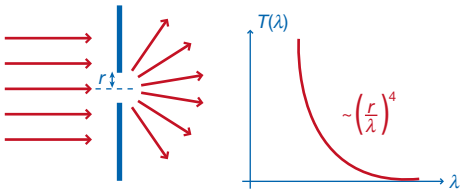

Box 1 Figure 1 | Diffraction and typical transmission spectrum of visible light through a subwavelength hole in an infinitely thin perfect metal film.

However, a real aperture is characterized by a depth and therefore has waveguide properties. The transmission of light through such a guide is very different from the propagation of light in empty space. The confined space of the waveguide essentially modifies the dispersion relation of the electromagnetic field. The lateral dimensions of the waveguide define the wavelength at which light can no longer propagate through the aperture. This wavelength is known as the cutoff wavelength λ_c. When the incident wavelength $\lambda > \lambda_c$ the transmission is exponentially small, characterizing the non-propagating regime as shown in Box 1 Fig. 2. With real metals, the cutoff wavelength cannot be sharply defined because one goes continuously from propagative to evanescent regime as the wavelength increases.

There is a straightforward relationship between the cross-section of the waveguide and λ_c. However, one should take into account that λ_c for an aperture in a real metal is increased by taking the skin-depth into account, reflecting the penetration of the electromagnetic field inside the walls of the metal waveguide. It is possible to control and even to eliminate cutoff wavelengths even when the lateral dimensions are much smaller than λ, by playing with more complex geometries. While simple apertures are always characterized by the existence of cutoff wavelengths, an annular hole, for example, which resembles a coaxial cable, has no cutoff wavelength and is always propagating. The polarization of the incident light is also an important parameter, and with non-cylindrical waveguides, the transmission can be made extremely polarization sensitive. A striking illustration is provided by a slit. Here, for incident polarization parallel to the long axis, the transmission can be made subwavelength, as soon as the short dimension of the rectangle is smaller than λ. However, for the perpendicular polarization, no matter how narrow the guide is, the light always propagates through it. This allows for many possibilities in the choice of geometry depending on the application.

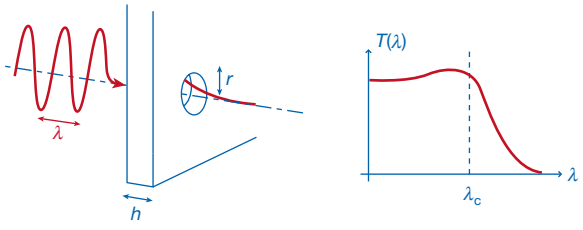

Box 1 Figure 2 | A cylindrical waveguide with a radius *r* much smaller than the wavelength λ of the incident electromagnetic field milled in a metal film of thickness *h*. The exponentially decreasing tail represents the attenuation of the subwavelength regime. A transmission spectrum can reveal the different propagating and evanescent regimes.

Box 2 | Coupling to SPs

At the interface separating a dielectric with a permittivity ε_d and a metal with a permittivity ε_m, SPs can be resonantly excited by the coupling between free surface charges of the metal and the incident electromagnetic field. Such a mode is characterized by a surface wave vector that obeys the following dispersion relation:

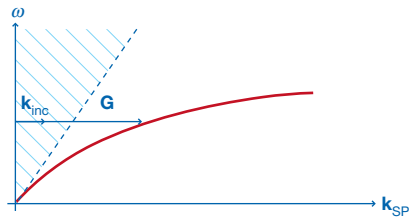

Box 2 Figure 1 | SP dispersion relation. The dotted line corresponds to the light line. The hatched sector of propagating waves does not overlap with the evanescent sector below the light line that fully contains the SP dispersion relation. $\mathbf{k}_{inc}$ is the transverse component of the incident wave vector and **G** corresponds to the momentum needed to couple to the SP mode in the evanescent sector.

$$k_{SP} = \frac{\omega}{c}\sqrt{\frac{\varepsilon_m \varepsilon_d}{\varepsilon_m + \varepsilon_d}}$$

Here, ω is the pulsation of the electromagnetic field and c the velocity of light in vacuum. Provided that the real part of ε_m is smaller than $-\varepsilon_d$, this wave vector has positive real and imaginary parts. The latter corresponds to the propagation length of the surface wave before it is damped inside the metal, and can be tens of micrometres at the smooth surface of noble metals, such as Au or Ag, at optical wavelengths. The real part of k_{SP} is plotted in Box 2 Fig. 1. It is always below the light line that separates free-space photons from evanescent ones. This implies immediately that such a mode is evanescent and therefore cannot be excited directly by freely propagating light. A given additional momentum **G** is needed to go from the propagating sector where the wave vector $\mathbf{k}_{inc}$ of the incident light falls to the evanescent one where SP modes exist. This is expressed in the simple resonance condition $\mathbf{k}_{SP} = \mathbf{k}_{inc} + \mathbf{G}$, which is a function of the incident pulsation and incident angle θ.

One way to provide the missing momentum **G** necessary for coupling incoming light to SPs is to use a periodic array. In one dimension for instance, it can be shown that **G** is related to multiples of $2\pi/a_0$ where a_0 is the period of the structure. This is the origin of the optical resonant behaviour of the array, because only when:

$$k_{SP} = k_0 \sin\theta + i \times \frac{2\pi}{a_0}$$

does light couple to SPs (i is an integer). The electromagnetic wave is then trapped momentarily on the surface, giving rise to the transmission peaks. The array generates a complex band structure, as schematically shown in Box 2 Fig. 2. At every multiple of π/a_0 (Brillouin zone edges), SPs are back-reflected so strongly that they cannot propagate any more. Bandgaps appear in the SP dispersion relation, corresponding to stationary waves and high field enhancements.

It should be noted that, when illuminated, non-periodic structures such as single holes, sharp edges, particles and so on can generate localized SP modes. This is possible when the dimensions of the defects are smaller than the wavelength of the incident field, generating a broad spectrum of **G** vectors (stemming from the spatial Fourier spectrum of the particular defect) in which a solution to the coupling condition $\mathbf{k}_{SP} = \mathbf{k}_{inc} + \mathbf{G}$ can be found. The coupling efficiency is dependent on the particular profile of the defect.

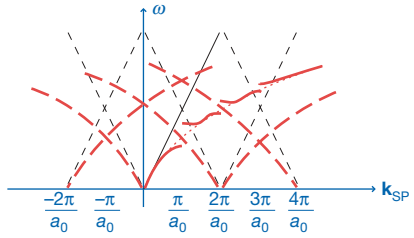

Box 2 Figure 2 | SP band structure on a periodic array.

subwavelength apertures below, the best transmission signals are obtained in noble metals such Au and Ag. To obtain detectable resonances at visible wavelengths, the dimensions of the holes should be of the order of 150 to 300 nm and the films not much thicker than 200 to 300 nm.

Small apertures are routinely used in SNOM tips to explore and to map with subwavelength resolution the electromagnetic field in the immediate vicinity of a surface[3]. More recently, tiny apertures have been implemented in fluorescence correlation spectroscopy[17–19], a powerful technique for the study of the diffusion and reaction of single fluorescent biomolecules in which the information is derived from the analysis of the statistical fluctuations of individual molecules as they move through a small volume. Traditionally, the volume is defined by the focal point of a laser beam, that is, about 1 μm^3, which puts a limit on the upper concentration that can be used while still observing statistical fluctuations. By using small apertures in metal (see Fig. 2)[18,19], the analysed volume has been reduced by a factor of 1,000, allowing one to study molecular events at nearly millimolar concentrations—closer to biological conditions. In addition, such structures give rise to other benefits: the localized SP fields increase the excitation rate of the molecules in its vicinity[10,14,19], the emission pattern is potentially directional[9,10] and the branching ratios from the fluorescent state are affected[19]. All these can lead to an increase in the detected signal, rendering fluorescence correlation spectroscopy ever more useful as a tool for biology.

Single apertures surrounded by periodic corrugations

With modern nanofabrication techniques it is possible to modify the optical properties of a single aperture by sculpting the surrounding material at the scale of the wavelength[20–28]. Such modifications give rise to much higher transmission than single holes at selected wavelengths and in addition, novel lensing effects including beaming can be induced by texturing the output surface of the aperture—as discussed next.

When a single aperture is surrounded by circular corrugations as shown in Fig. 3a, the periodic structure acts like an antenna to couple the incident light into SPs at a given λ. As a consequence the electromagnetic fields at the surface become intense above the aperture, resulting in very high transmission efficiencies and a well-defined spectrum (Fig. 3a). Here the resonant wavelength is mainly determined by the periodicity of the grooves, which provides the necessary momentum and energy-matching conditions (as explained in Box 2). The resonance is, however, slightly more red-shifted than the period owing to the interaction with the light directly transmitted through the hole. This should be considered in tuning the structure to be bright at a desired wavelength. When such a structure is milled in a metal like Ag, the value of η can be much larger than one[21]. Again, absolute quantification is difficult, but compared to a bare single hole of the same dimensions the transmission gain can be an order of magnitude at resonant wavelengths[20]. This, as we shall see below, has important applications.

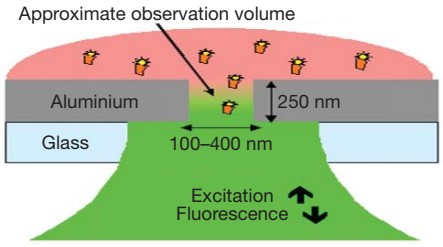

Figure 2 | Schematic diagram of the fluorescence correlation spectroscopy in a single hole. The fluorescence of individual molecules is collected as they diffuse through the observation volume defined by the hole in the metal film. The fluorescence is collected from the same side as the incident excitation. Courtesy of J. Wenger.

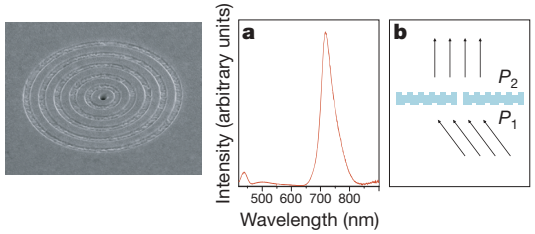

Figure 3 | Optical properties of single apertures surrounded by periodic corrugations. **a**, Transmission spectrum of a single hole surrounded by periodic corrugations (left) prepared by focused ion beam (hole diameter 300 nm, period 650 nm). **b**, Schematic illustration of redirecting beam by single-slit aperture surrounded by grooves of different periodicity on the input (P_1) and output (P_2) surfaces.

If the output surface surrounding the aperture is also corrugated, a surprisingly narrow beam can be generated, having a divergence of less than a few degrees[20], which is far smaller than that of the single apertures discussed earlier. This is because the light emerging from the hole couples to the periodic structure of the exit surface and to the modes existing in the grooves—which in turn scatter the surface waves into freely propagating light[22–24]. This then interferes with the light that has travelled directly through the hole generating the focused beam. A variant of the double-sided bull's-eye structure is a slit with parallel grooves on both sides of the film, which in addition disperses light spatially according to wavelength[20,28]. Such double-sided structures act as a novel kind of optical element[20,23–25]. They can have a focal plane like a lens but at the same time have other unusual features. For instance, by having grooves with different periods on either side of the film next to a slit, the direction of the output beam can be made independent of the input beam, unlike conventional lenses or gratings, suggesting many practical applications (Fig. 3b). This ability to redirect the beam stems from the way input and output corrugations act like two separate independent gratings connected by a pinhole.

The antenna capacity of the corrugations to concentrate the photons at the tiny central aperture also opens up other technological possibilities such as a bright subwavelength spot for ultradense optical-data storage and nonlinear phenomena[29–31]. Of paramount importance to modern optical telecommunication are photodetectors that can translate an optical signal into an electrical one and thereby convert the flow of information being carried through the telecom network into a displayable signal on the screen. Such photodetectors must therefore be as fast as possible to handle the large amount of data flow. Typically the operating speed of a photodetector scales inversely with the size of its photoelectrical element, but the size cannot be made too small because then it would no longer collect enough photons. To circumvent this problem, an ultrafast photodetector has been realized that elegantly combines a very small photoelectrical element with a bull's-eye antenna structure (shown in Fig. 4) that collects and concentrates the incoming photons[32]. This combination illustrates well the potential benefit of plasmonic devices for optoelectronics.

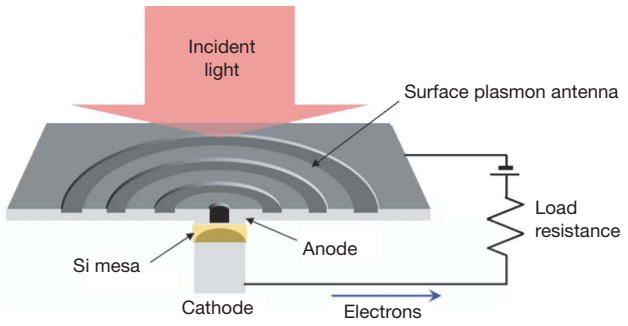

Figure 4 | Ultrafast miniature photodetector. This device consists of a small Si photoelectric element and a SP antenna (reproduced from ref. 32 with permission). The incoming light is harvested by the periodic structure surrounding the central hole, which then transmits it to the underlying photodetector.

Hole arrays

Periodic arrays of holes in an opaque metal film have so far been the structures that have found the most applications owing to the simplicity with which their spectral properties can be tuned and scaled. Among other things, they can act as filters for which the transmitted colour can be selected by merely adjusting the period. As we saw in the previous section (and Box 2), periodic metallic structures can convert light into SPs by providing the necessary momentum conservation for the coupling process. It is therefore not surprising that periodic arrays of holes such as those shown in Fig. 5 can give rise to the extraordinary transmission phenomenon[4] where the transmission spectrum contains a set of peaks with η larger than one even when the individual holes are so small that they do not allow propagation of light (Fig. 5). Hole arrays have been characterized in great detail both theoretically[33–59] and experimentally[58–79]. As in the case of single holes surrounded by periodic grooves[22], the process can be divided into three steps: the coupling of light to SPs on the incident surface, transmission through the holes to the second surface and then re-emission from the second surface. At the peak transmissions, standing SP waves are formed on the surface (Box 2). The intensity of SP electromagnetic fields above each hole compensates for the otherwise inefficient transmission through each individual hole (Box 1).

If we apply the momentum-matching conditions discussed in Box 2 to a two-dimensional triangular array shown in Fig. 5, we can show that the peak positions λ_{max} at normal incidence are given in a first approximation by:

$$\lambda_{max} = \frac{P}{\sqrt{\frac{4}{3}(i^2+ij+j^2)}}\sqrt{\frac{\varepsilon_m\varepsilon_d}{\varepsilon_m+\varepsilon_d}} \qquad (2)$$

where P is the period of the array, ε_m and ε_d are respectively the dielectric constants of the metal and the dielectric material in contact with the metal and i, j are the scattering orders of the array. Because equation (2) does not take into account the presence of the holes and the associated scattering losses, it neglects the interference that gives rise to a resonance shift[42,43]. As a consequence, it predicts peak positions at wavelengths slightly shorter than those observed experimentally, as can be seen in Fig. 5.

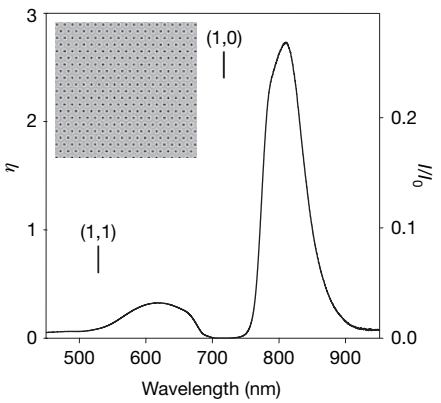

Figure 5 | Transmission spectrum of hole arrays. The triangular hole array was milled in a 225-nm-thick Au film on a glass substrate with an index-matching liquid on the air side (hole diameter 170 nm, period 520 nm). The transmission spectrum is measured at normal incidence using collimated white light. The inset shows the image of the actual array. I/I_o is the absolute transmission of the array and η is the same transmission but normalized to the area occupied by the holes.

Implicit in the resonance conditions defined by equations such as equation (2) are the symmetry relations of the array. Therefore the SPs generated in the array will propagate along defined symmetry axes with their own polarization depending on the (i, j) number of the mode. This results in a rich polarization behaviour that can be revealed in particular under focused light illumination[79].

We emphasize that both surfaces on either side of the holes can sustain SP modes offset from each other by the difference in ε_d of the material in immediate contact with the metal surface (typically glass and air), as predicted by equation (2). Hence, the transmission spectrum of asymmetric structures contains two sets of peaks, each set belonging to one of the surfaces. In many applications, hole arrays of a finite size are used for practical reasons. If the arrays contain small numbers of holes then the periodicity is not well defined and the contribution from the edges becomes significant, changing the spectrum and leading to unusual re-emission patterns[33].

One interesting feature of hole arrays is the fact that each hole on the output surface acts like a new point source for the light. Therefore, if a plane wave (that is, a collimated beam) impinges on the input surface, then a plane wave is reconstructed through classical interference as the light travels away from the output surface. Naturally, because the array is also a grating, the transmission gives rise to different diffraction orders depending on the wavelength to period ratio. For the longest-wavelength (1,0) peak shown in Fig. 5, only the 0th order diffraction is formed, because $\lambda > P$. When $\lambda < P$, higher diffraction orders gradually appear as the wavelength becomes shorter.

The shape and dimensions of the holes in an array do influence its transmission spectrum[64,65]. For instance, in the case of non-propagative apertures, switching from circular to rectangular holes changes the spectrum as a result of the simultaneous change in both the localized SP mode associated with each individual hole and the cutoff wavelength (the wavelength above which the aperture no longer allows light propagation; see Box 1). Nevertheless, the spectrum is dominated by the SP modes because of the periodicity of the array[65]. If the transmission peak falls below the cutoff, its intensity drops exponentially with the depth of the hole and hence the film thickness (or hole depth) is a critical parameter in these structures[33]. It should be noted that arrays of slits have more complex transmission spectra than do hole arrays because the slits can be made propagative under the appropriate polarization (Box 1). As a consequence, the transmission spectra typically contain the signature of both cavity modes in the slits (often at wavelengths that equal twice the slit depth divided by an integer) and SP modes, owing to the slit periodicity[35,48–54,61].

Hole arrays have many applications, from optical elements to sensors for chemistry and biology. For instance, the array acts like a tunable filter because the wavelength selectivity of the array transmission can be adjusted simply by changing the period, as predicted by equation (2) and illustrated in Fig. 6. The letters 'hν' are obtained by fabricating a periodic dimple array in which some of the dimples are milled through to form holes, which in turn reveal the spectral signature of the array.

The combination of the large electromagnetic fields generated by the SPs on the hole arrays, their sensitivity to the dielectric medium in contact with the surface (equation (2)) and the simplicity of the arrays have spurred efforts to use them to detect molecules and to enhance spectroscopic signals (fluorescence, Raman and so on)[80–89]. In this perspective, the enhanced infrared molecular vibrational spectroscopy exemplifies well the usefulness of the hole arrays for chemistry and biology[80]. Arrays of square holes in a Ni film with a periodicity tuned to the infrared were prepared and modified with Cu oxide to induce the catalytic transformation of methanol to formaldehyde on the surface. When such an array with a single adsorbed molecular layer on surface is placed in a Fourier-transform infrared apparatus, the infrared vibrational absorption spectrum (Fig. 7) that is extracted is at least 100 times stronger than if the apparatus had probed a molecular layer on an inert dielectric substrate[80,87]. The large signal enhancement is due to the fact that when the light is trapped momentarily on the surface in terms of SPs, its interaction time with the molecules increases and therefore so does the probability of the absorption. Note that absorption enhancement of electronic transitions is also observed in the visible part of the spectrum, although the enhancement factor is then only a factor of ten, owing to the shorter SP lifetime on the surface at optical wavelengths[90]. Needless to say, such results are extremely promising for studying molecular monolayers and surface reactions by static or time-resolved spectroscopy because this method provides a much better signal-to-noise ratio and is relatively easy to implement.

Other considerations for optimizing apertures

So far we have discussed mainly the broad features associated with tiny holes in opaque metal films. The unique properties of these holes being related to the presence of SPs, they are in turn very much dependent on geometric factors and the properties of the metal.

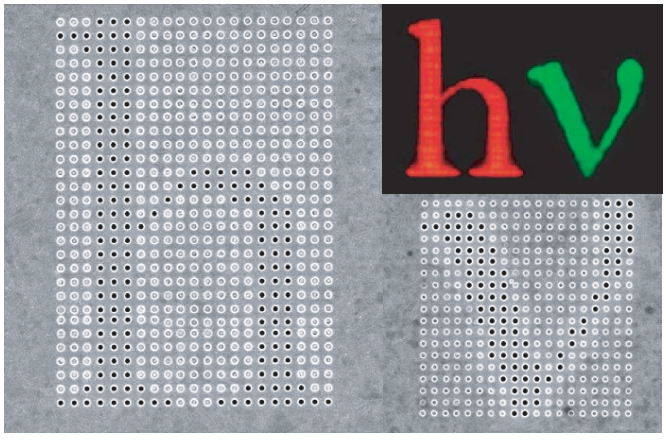

Figure 6 | Holes in a dimple array generating the letters 'hν' in transmission. An array of dimples is prepared by focused-ion-beam milling an Ag film. Some of the dimples are milled through to the other side so that light can be transmitted. When this structure is illuminated with white light, the transmitted colour is determined by the period of the array. In this case the periods were chosen to be 550 and 450 nm respectively to achieve the red and green colours.

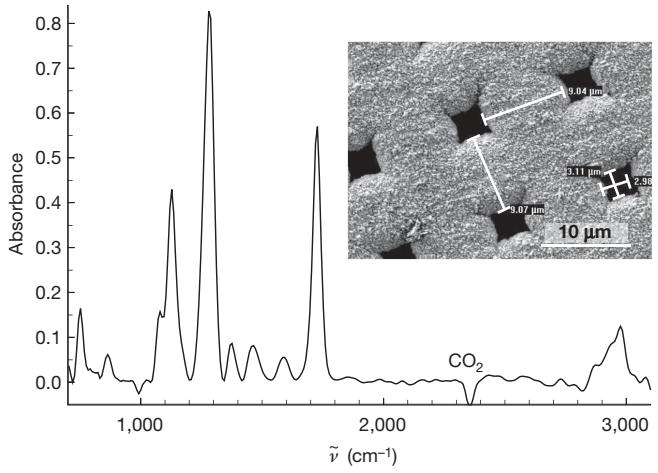

Figure 7 | Infrared enhanced vibrational spectra. Vibrational absorption spectrum of formaldehyde (CH_2O) monolayer adsorbed on a Ni hole array covered with Cu oxide (adapted from ref. 81 with permission). Note that absorbance of 0.8 implies that 84% of the incident light is absorbed by the molecular monolayer. The Ni hole array here acts like the antenna, trapping the light momentarily on the surface and therefore increasing the likelihood of absorption by the CH_2O.

The choice of the metal depends on the wavelength to be used because the dielectric constants of metals are wavelength dependent. Ideally, the dielectric constant of the metal should have a high absolute value for the real part and a small imaginary part that determines the absorption into the metal. This combination gives rise to high SP fields at the surface and minimizes the losses. Therefore Ag is ideally suited to obtain high transmission in the visible part of the spectrum, while above 600 nm Au is even better because it suffers little oxidation. In the infrared, metals such as Ni or Cu can also be used.

Interestingly, high transmittivity through structures similar to those described above but scaled to the microwave region of the spectrum have also been reported where SPs are not considered to exist[91–95]. This is explained by the fact that when a metal surface is corrugated, it is the effective dielectric constant that is modified rather than the bulk metal[37] (this is similar to the way the wetting properties of a material are changed by nanostructuring). As a consequence, SP-like surface waves (also known as 'spoof plasmons') are formed, which enhances the transmittivity[94,95]. More generally, it is essential to trap the electromagnetic wave in the vicinity of the aperture to observe enhanced transmission and its related phenomena. We therefore expect that surface waves such as surface phonon polaritons can also be used. There has been some discussion on whether SPs are involved in the optical transmission of aperture structures but a recent analysis has confirmed the key role of SPs[96,97], in agreement with the vast majority of studies.

The geometrical factors that influence the optical properties of the holes are numerous: symmetry of the structure, the aspect ratios and shape of the holes, aperture area, profile of the corrugations and so forth. These variables determine the electromagnetic field distribution on the surface, the propagation dynamics of the surface waves and their scattering efficiencies, and, the in-plane and out-of-plane coupling to light. The depth of the holes (or thickness of the metal film) is important for several reasons. If the films are too thin, they are partially transparent to the incident light and no holes are necessary to achieve significant transmission, especially if the surfaces are in addition resonantly corrugated[98,99]. To obtain a large contrast between the aperture brightness and the surrounding metal, the metal must be opaque (optically thick), which implies that the film thickness must be several times the skin-depth of the metal. The skin-depth is the penetration depth in the metal at which incoming light intensity has been reduced by $1/e$. Typical skin-depths are of the order of 20 nm for noble metals in the visible spectrum, so film thicknesses of the order of 200 nm are appropriate at optical wavelengths. Even in such thick films, the surface modes on either side of a metal film can also interact via the holes, split and give rise to modes with new energies. Such an effect is especially visible in hole arrays and disappears as the film thickness increases and the modes on either side are decoupled[33,37].

There are many ways to fabricate aperture structures, depending on the scale of interest. For the optical regime, the techniques of choice are: focused ion beam, electron beam lithography and photolithography. The latter two involve several steps but are particularly useful for large-scale structures. The focused ion beam technique, in which the sample is milled by focused ion bombardment, is ideally suited for texturing the metal surface, for instance when preparing grooves around an aperture. Finally, care is needed in preparing the metal films because their quality is an important parameter in the optical properties of the structure.

Potential applications

Surface-wave-activated holes in metal films are finding applications well beyond the illustrations given in the above paragraphs. In the field of opto-electronics for instance, studies are being carried out to extract more light from light-emitting devices[100]. The metal electrodes of such devices, which are normally a source of loss, can be structured with holes to help extract the light from the diode. The need for ever-smaller features on electronic chips is pushing photolithography to use shorter wavelengths, with the associated increased costs and complications. The use of extraordinary optical transmission could perhaps circumvent this problem by using SP-activated lithography masks, which allow subwavelength features in the near-field and high throughput[101–103].

The combination of molecules and holes is another promising area of application, whether for the realization of devices or for the spectroscopic purposes illustrated above. The high optical contrast of SP-activated holes, their small sizes and their simplicity make them ideal candidates for integration on biochips as sensing elements. As in all SP-enhanced phenomena, both the input and output optical fields can be strengthened, with the additional feature that the structure can potentially focus the signal towards a detector. For the purpose of making SP-active devices, the transmission of hole arrays can be switched by controlling the refractive index of molecular materials either electrically[104] or optically up to terahertz speeds[105].

Finally, subwavelength holes might find use in quantum and atom optics. For instance, hole arrays are promising tools in the study of the physical nature—quantum versus classical—of SPs as collective excitations when implemented in quantum entanglement experiments[106,107]. It has been shown theoretically that the extraordinary transmission phenomenon can also be expected for matter waves involving ultracold atoms[108] such as those used in Bose–Einstein condensates. This presents opportunities to create optical elements to manipulate atoms and control their direction.

The potential of the optics of tiny holes in metal screens lies in the contrast between the strong opacity of the metal and the aperture, combined with the fact that the metal allows for high local field enhancements. In addition, the properties of these apertures can be tailored by structuring the metal with modern nanofabrication techniques. The simplicity of the structures and their ease of use should further expand their application in a variety of areas and lead to unsuspected developments.

1. Grimaldi, F.-M. in *Physico-mathesis de Lumine, Coloribus, et Iride, Aliisque Sequenti Pagina Indicatis* 9 (Bologna, 1665).
2. Bethe, H. A. Theory of diffraction by small holes. *Phys. Rev.* **66,** 163–182 (1944).
3. Betzig, E. & Trautman, J. K. Near-field optics: microscopy, spectroscopy, and surface modification beyond the diffraction limit. *Science* **257,** 189–194 (1992).
4. Ebbesen, T. W., Lezec, H. J., Ghaemi, H. F., Thio, T. & Wolff, P. A. Extraordinary optical transmission through sub-wavelength hole arrays. *Nature* **391,** 667–669 (1998).
5. Ritchie, R. H. Plasma losses by fast electrons in thin films. *Phys. Rev.* **106,** 874–881 (1957).
6. Barnes, W. L., Dereux, A. & Ebbesen, T. W. Surface plasmon subwavelength optics. *Nature* **424,** 824–830 (2003).
7. Roberts, A. Electromagnetic theory of diffraction by a circular aperture in a thick, perfectly conducting screen. *J. Opt. Soc. Am. A* **4,** 1970–1983 (1987).
8. Gordon, R. & Brolo, A. Increased cut-off wavelength for a subwavelength hole in a real metal. *Opt. Express* **13,** 1933–1938 (2005).
9. Obermüller, C. & Karrai, K. Far-field characterization of diffracting apertures. *Appl. Phys. Lett.* **67,** 3408–3410 (1995).
10. Degiron, A., Lezec, H. J., Yamamoto, N. & Ebbesen, T. W. Optical transmission properties of a single subwavelength aperture in a real metal. *Opt. Commun.* **239,** 61–66 (2004).
11. Yin, L. *et al.* Surface palsmons at single nanoholes in Au films. *Appl. Phys. Lett.* **85,** 467–469 (2004).
12. Garcia-Vidal, F. J., Moreno, E., Porto, J. A. & Martin-Moreno, L. Transmission of light through a single rectangular hole. *Phys. Rev. Lett.* **95,** 103901 (2005).
13. Chang, C.-W., Sarychev, A. K. & Shalaev, V. M. Light diffraction by a subwavelength circular aperture. *Laser Phys. Lett.* **2,** 351–355 (2005).
14. Popov, E. *et al.* Surface plasmon excitation on a single subwavelength hole in a metallic sheet. *Appl. Opt.* **44,** 2332–2337 (2005).
15. Webb, K. J. & Li, J. Analysis of transmission through small apertures in conducting films. *Phys. Rev. B* **73,** 033401 (2006).
16. Garcia de Abajo, F. J. Light transmission through a single cylindrical hole in a metallic film. *Opt. Express* **10,** 1475–1484 (2002).
17. Magde, D., Elson, E. & Webb, W. W. Thermodynamic fluctuations in a reacting system - measurement by fluorescence correlation spectroscopy. *Phys. Rev. Lett.* **29,** 705–707 (1972).
18. Levene, M. J. *et al.* Zero-mode waveguides for single molecule analysis at high concentrations. *Science* **299,** 682–686 (2003).
19. Rignault, H. *et al.* Enhancement of single-molecule fluorescence detection in subwavelength apertures. *Phys. Rev. Lett.* **95,** 117401 (2005).

20. Lezec, H. J. *et al.* Beaming light from a subwavelength aperture. *Science* **297,** 820–822 (2002).
21. Thio, T., Pellerin, K. M., Linke, R. A., Lezec, H. J. & Ebbesen, T. W. Enhanced light transmission through a single subwavelength aperture. *Opt. Lett.* **26,** 1972–1974 (2001).
22. Degiron, A. & Ebbesen, T. W. Analysis of the transmission process through single apertures surrounded by periodic corrugations. *Opt. Express* **12,** 3694–3700 (2004).
23. Martin-Moreno, L., Garcia-Vidal, F. J., Lezec, H. J., Degiron, A. & Ebbesen, T. W. Theory of highly directional emission from a single subwavelength aperture surrounded by surface corrugations. *Phys. Rev. Lett.* **90,** 167401 (2003).
24. Garcia-Vidal, F. J., Lezec, H. J., Ebbesen, T. W. & Martin-Moreno, L. Multiple paths to enhance optical transmission through a subwavelength slit. *Phys. Rev. Lett.* **90,** 213901 (2003).
25. Garcia-Vidal, F. J., Martin-Moreno, L., Lezec, H. J. & Ebbesen, T. W. Focusing light with a single subwavelength aperture flanked by surface corrugations. *Appl. Phys. Lett.* **83,** 4500–4502 (2003).
26. Yu, L.-B. *et al.* Physical origin of directional beaming from a subwavelength slit. *Phys. Rev. B* **71,** 041405(R) (2005).
27. Ishi, T., Fujikata, J. & Ohashi, K. Large optical transmission through a single subwavelength hole associated with a sharp-apex grating. *Jpn J. Appl. Phys.* **44,** L170–L172 (2005).
28. Sun, Z. & Kim, H. K. Refractive transmission of light and beam shaping with metallic nano-optics lenses. *Appl. Phys. Lett.* **85,** 642–644 (2004).
29. Gbur, G., Schouten, H. F. & Visser, T. D. Achieving superresolution in near-field optical data readout systems using surface plasmons. *Appl. Phys. Lett.* **87,** 191109 (2005).
30. Fujikata, J. *et al.* Surface plasmon enhancement effect and its application to near-field optical recording. *Trans. Magn. Soc. Jpn* **4,** 255–259 (2004).
31. Nahata, A., Linke, R. A., Ishi, T. & Ohashi, K. Enhanced nonlinear optical conversion from a periodically nanostructured metal film. *Opt. Lett.* **28,** 423–425 (2003).
32. Ishi, T., Fujikata, J., Makita, K., Baba, T. & Ohashi, K. Si nano-photodiode with a surface plasmon antenna. *Jpn J. Appl. Phys.* **44,** L364–L366 (2005).
33. Degiron, A., Lezec, H. J., Barnes, W. L. & Ebbesen, T. W. Effects of hole depth on enhanced light transmission through subwavelength hole arrays. *Appl. Phys. Lett.* **81,** 4327–4329 (2002).
34. Bravo-abad, J. *et al.* How light emerges from an illuminated array of subwavelength holes. *Nature Phys.* **2,** 120–123 (2006).
35. Porto, J. A., Garcia-Vidal, F. J. & Pendry, J. B. Transmission resonances on metalllic gratings with very narrow slits. *Phys. Rev. Lett.* **83,** 2845–2848 (1999).
36. Strelniker, Y. M. & Bergman, D. J. Optical transmission through metal films with a subwavelength hole array in the presence of a magnetic field. *Phys. Rev. B* **59,** R12763 (1999).
37. Martin-Moreno, L. *et al.* Theory of extraordinary optical transmission through subwavelength hole arrays. *Phys. Rev. Lett.* **86,** 1114–1117 (2001).
38. Popov, E., Neviere, M., Enoch, S. & Reinisch, R. Theory of light transmission through subwavelength periodic hole arrays. *Phys. Rev. B* **62,** 16100 (2000).
39. Barbara, A., Quemerais, P., Bustarret, E. & Lopez-Rios, T. Optical transmission through subwavelength metallic gratings. *Phys. Rev. B* **66,** 161403(R) (2002).
40. Baida, F. I. & Van Labeke, D. Light transmission by subwavelength annular aperture arrays in metallic films. *Opt. Commun.* **209,** 17–22 (2002).
41. Sarychev, A. K., Podolskiy, V. A., Dykhne, A. M. & Shalaev, V. M. Resonance transmittance through a metal film with subwavelength holes. *IEEE J. Quant. Elect.* **38,** 956–963 (2002).
42. Sarrazin, M., Vigneron, J. P. & Vigoureux, J.-M. Role of Wood anomalies in optical properties of thin metallic films with a bidimensional array of subwavelength holes. *Phys. Rev. B* **67,** 085415 (2003).
43. Genet, C., van Exter, M. P. & Woerdman, J. P. Fano-type interpretation of red shifts and red tails in hole array transmission spectra. *Opt. Commun.* **225,** 331–336 (2003).
44. Zayats, A. V., Salomon, L. & de Fornel, F. How light gets through periodically nanostructured metal films: a role of surface polaritonic crystals. *J. Microsc.* **210,** 344–349 (2003).
45. Lalanne, P., Rodier, J. C. & Hugonin, J. P. Surface plasmons of metallic surfaces perforated by nanohole arrays. *J. Opt. Pure Appl. Opt.* **7,** 422–426 (2005).
46. Lomakin, V. & Michielssen, E. Enhanced transmission through metallic plates perforated by arrays of subwavelength holes and sandwiched between dielectric slabs. *Phys. Rev. B* **71,** 235117 (2005).
47. Müller, R., Malyarchuk, V. & Lienau, C. Three-dimensional theory on light-induced near-field dynamics in a metal film with a periodic array of nanoholes. *Phys. Rev. B* **68,** 205415 (2003).
48. Takakura, Y. Optical resonance in a narrow slit in a thick metallic screen. *Phys. Rev. Lett.* **86,** 5601–5603 (2001).
49. Shipman, S. P. & Venakides, S. Resonant transmission near nonrobust periodic slab modes. *Phys. Rev. E* **71,** 026611 (2005).
50. Shen, J. T., Catrysse, P. B. & Fan, S. Mechanism for designing metallic metamaterials with a high index of refraction. *Phys. Rev. Lett.* **94,** 197401 (2005).
51. Xie, Y., Zakharian, A. R., Moloney, J. V. & Mansuripur, M. Transmission of light through slit apertures in metallic films. *Opt. Express* **12,** 6106–6121 (2004).
52. Lee, K. G. & Park, Q.-H. Coupling of surface plasmon polaritons and light in metallic nanoslits. *Phys. Rev. Lett.* **95,** 103902 (2005).
53. Marquier, F., Greffet, J.-J., Collin, S., Pardo, F. & Pelouard, J. L. Resonant transmission through metallic film due to coupled modes. *Opt. Express* **13,** 70–76 (2005).
54. Skigin, D. C. & Depine, R. A. Transmission resonances of metallic compound gratings with subwavelength slits. *Phys. Rev. Lett.* **95,** 217402 (2005).
55. Kim, K. Y., Cho, Y. K., Tae, H. S. & Lee, J.-H. Light transmission along dispersive plasmonic gap and its subwavelength guidance characteristics. *Opt. Express* **14,** 320–330 (2006).
56. Liu, W.-C. & Tsai, D. P. Optical tunnelling effect of surface plasmon polaritons and localized surface plasmon resonance. *Phys. Rev. B* **65,** 155423 (2005).
57. Garcia de Abajo, F. J., Saenz, J. J., Campillo, I. & Dolado, J. S. Site and lattice resonances in metallic hole arrays. *Opt. Express* **14,** 7–18 (2006).
58. Chang, S.-H., Gray, S. K. & Schatz, G. C. Surface plasmon generation and light transmission by isolated nanoholes and arrays of nanoholes in thin metal films. *Opt. Express* **13,** 3150–3165 (2005).
59. Bravo-Abad, J., Garcia-Vidal, F. J. & Martin-Moreno, L. Resonant transmission of light through finite chains of subwavelength holes in a metallic film. *Phys. Rev. Lett.* **93,** 227401 (2005).
60. Ghaemi, H. F., Thio, T., Grupp, D. E., Ebbesen, T. W. & Lezec, H. J. Surface plasmons enhance optical transmission through subwavelength holes. *Phys. Rev. B* **58,** 6779–6782 (1998).
61. Sun, Z., Jung, Y. S. & Kim, H. K. Role of surface plasmons in the optical interaction in metallic gratings with narrow slits. *Appl. Phys. Lett.* **83,** 3021–3023 (2003).
62. Barnes, W. L., Murray, W. A., Dintinger, J., Devaux, E. & Ebbesen, T. W. Surface plasmon polaritons and their role in the enhanced transmission of light through periodic arrays of sub-wavelength holes in a metal film. *Phys. Rev. Lett.* **92,** 107401 (2004).
63. Prikulis, J., Hanarp, P., Olofsson, L., Sutherland, D. & Kall, M. Optical spectroscopy of nanometric holes in thin gold films. *Nano Lett.* **4,** 1003–1007 (2004).
64. Klein Koerkamp, K. J., Enoch, S., Segerink, F. B., van Hulst, N. F. & Kuipers, L. Strong influence of hole shape on extraordinary transmission through periodic arrays of subwavelength holes. *Phys. Rev. Lett.* **92,** 183901 (2004).
65. Degiron, A. & Ebbesen, T. W. The role of localized surface plasmon modes in the enhanced transmission of periodic subwavelength apertures. *J. Opt. Pure Appl. Opt.* **7,** S90–S96 (2005).
66. Gordon, R. *et al.* Strong polarization in the optical transmission through elliptical nanohole arrays. *Phys. Rev. Lett.* **92,** 037401 (2004).
67. Ye, Y.-H. & Zhang, J.-Y. Enhanced light transmission through cascaded metal films perforated with periodic hole arrays. *Opt. Lett.* **30,** 1521–1523 (2005).
68. Krasavin, A. V. *et al.* Polarization conversion and "focusing" of light propagating through a small chiral hole in a metallic screen. *Appl. Phys. Lett.* **86,** 201105 (2005).
69. Wang, Q.-J., Li, J.-Q., Huang, C.-P., Zhang, C. & Zhu, Y.-Y. Enhanced optical transmission through metal films with rotation-symmetrical hole arrays. *Appl. Phys. Lett.* **87,** 091105 (2005).
70. Ropers, C. *et al.* Femtosecond light transmission and subradiant damping in plasmonic crystals. *Phys. Rev. Lett.* **94,** 113901 (2005).
71. Dogariu, A., Thio, T., Wang, L. J., Ebbesen, T. W. & Lezec, H. J. Delay in light transmission through small apertures. *Opt. Lett.* **26,** 450–452 (2001).
72. Halté, V., Benabbas, A., Guidoni, L. & Bigot, J.-Y. Femtosecond dynamics of the transmission of gold arrays of subwavelength holes. *Phys. Status Solidi (b)* **242,** 1872–1876 (2005).
73. Dechant, A. & Elezzabi, A. Y. Femtosecond optical pulse propagation in subwavelength metallic slits. *Appl. Phys. Lett.* **84,** 4678–4680 (2004).
74. Kwak, E.-S. *et al.* Surface plasmon standing waves in large-area subwavelength hole arrays. *Nano Lett.* **5,** 1963–1967 (2005).
75. Kim, D. S. *et al.* Microscopic origin of surface-plasmon radiation in plasmonic band-gap nanostructures. *Phys. Rev. Lett.* **91,** 143901 (2003).
76. Egorov, D., Dennis, B. S., Blumberg, G. & Haftel, M. I. Two-dimensional control of surface plasmons and directional beaming from arrays of subwavelength apertures. *Phys. Rev. B* **70,** 033404 (2004).
77. Chyan, J. Y., Chang, C. A. & Yeh, J. A. Development and characterization of a broad-bandwidth polarization-insensitive subwavelength optical device. *Nanotechnology* **17,** 40–44 (2006).
78. Schouten, H. F. *et al.* Plasmon-assisted two-slit transmission: Young's experiment revisited. *Phys. Rev. Lett.* **94,** 053901 (2005).
79. Altewischer, E., van Exter, M. P. & Woerdman, J. P. Polarization analysis of propagating surface plasmons in a subwavelength hole array. *J. Opt. Soc. Am. B* **20,** 1927–1931 (2003).
80. Williams, S. M. *et al.* Use of the extraordinary infrared transmission of metallic subwavelength arrays to study the catalyzed reaction of methanol to formaldehyde on copper oxide. *J. Phys. Chem. B* **108,** 11833–11837 (2004).
81. Brolo, A. G. *et al.* Enhanced fluorescence from arrays of nanoholes in a gold film. *J. Am. Chem. Soc.* **127,** 14936–14941 (2005).
82. Liu, Y., Bishop, J., Williams, L., Blair, S. & Herron, J. Biosensing based upon molecular confinement in a metallic nanocavity arrays. *Nanotechnology* **15,** 1368–1374 (2004).
83. Brolo, A. G., Gordon, R., Leathem, B. & Kavanagh, K. L. Surface plasmon sensor based on the enhanced light transmission through arrays of nanoholes in gold films. *Langmuir* **20,** 4813–4815 (2004).
84. Moran, C. E., Steele, J. M. & Halas, N. J. Chemical and dielectric manipulation of plasmonic band gap of metallodielectric arrays. *Nano Lett.* **4,** 1497–1500 (2004).

85. Stark, P. R. H., Halleck, A. E. & Larson, D. N. Short order nanohole arrays in metals for highly sensitive probing of local indices of refraction as the basis for a highly multiplexed biosensor technology. *Methods* **37,** 37–47 (2005).
86. Brolo, A. G., Arctander, E., Gordon, R., Leathem, B. & Kavanagh, K. L. Nanohole-enhanced Raman scattering. *Nano Lett.* **4,** 2015–2018 (2004).
87. Williams, S. M. *et al.* Scaffolding for nanotechnology: extraordinary infrared transmission of microarrays for stacked sensors and surface spectroscopy. *Nanotechnology* **15,** S495–S503 (2004).
88. Coe, J. V. *et al.* Extra IR transmission with metallic arrays of subwavelength holes. *Anal. Chem.* **78,** 1385–1389 (2006).
89. Rindzevicius, T. *et al.* Plamsonic sensing characteristics of single nanometric holes. *Nano Lett.* **5,** 2335–2339 (2005).
90. Dintinger, J., Klein, S. & Ebbesen, T. W. Molecule–surface plasmon interactions in hole arrays: enhanced absorption, refractive index changes and all-optical switching. *Adv. Mat.* **18,** 1267–1270 (2006).
91. Gomez Rivas, J., Schotsch, C., Haring Bolivar, P. & Kurz, H. Enhanced transmission of Thz radiation through subwavelength holes. *Phys. Rev. B* **68,** 201306(R) (2003).
92. Shou, X., Agrawal, A. & Nahata, A. Role of metal thickness on the enhanced transmission properties of a periodic array of subwavelength apertures. *Opt. Express* **13,** 9834–9840 (2005).
93. Lockyear, M. J., Hibbins, A. P. & Sambles, J. R. Surface-topography-induced enhanced transmission and directivity of microwave radiation through a subwavelength circular metal aperture. *Appl. Phys. Lett.* **84,** 2040–2042 (2004).
94. Pendry, J. B., Martin-Moreno, L. & Garcia-Vidal, F. J. Mimicking surface plasmons with structured surfaces. *Science* **305,** 847–848 (2004).
95. Garcia-Vidal, F. J., Martin-Moreno, L. & Pendry, J. B. Surfaces with holes in them: new plasmonic metamaterials. *J. Opt. Pure Appl. Opt.* **7,** S97–S101 (2005).
96. Lalanne, P. & Hugonin, J. P. Interaction between optical nano-objects at metallo-dielectric interfaces. *Nature Phys.* **2,** 551–556 (2006).
97. Visser, T. D. Surface plasmons at work? *Nature Phys.* **2,** 509–510 (2006).
98. Gruhlke, R., Hod, W. & Hall, D. Surface-plasmon cross coupling in molecular fluorescence near a corrugated thin film. *Phys. Rev. Lett.* **56,** 2838–2841 (1986).
99. Bonod, N., Enoch, S., Li, L., Popov, E. & Nevière, M. Resonant optical transmission through thin metallic films with and without holes. *Opt. Express* **11,** 482–490 (2003).
100. Liu, C., Kamaev, V. & Vardeny, Z. V. Efficency enhancement of an organic light-emitting diode with a cathode forming two-dimensional periodic hole array. *Appl. Phys. Lett.* **86,** 143501 (2005).
101. Srituravanich, W., Fang, N., Sun, C., Luo, Q. & Zhang, X. Plasmonic nanolithography. *Nano Lett.* **4,** 1085–1088 (2004).
102. Luo, X. & Ishihara, T. Sub-100nm photolithography based on plasmon resonance. *Jpn J. Appl. Phys.* **43,** 4017–4021 (2004).
103. Shao, D. B. & Che, S. C. Surface-plasmon-assisted nanoscale photolithography by polarized light. *Appl. Phys. Lett.* **86,** 253107 (2005).
104. Kim, T. J., Thio, T., Ebbesen, T. W., Grupp, D. E. & Lezec, H. J. Control of optical transmission through metals perforated with subwavelength hole arrays. *Opt. Lett.* **24,** 256–258 (1999).
105. Dintinger, J., Robel, I., Kamat, P. V., Genet, C. & Ebbesen, T. W. Terahertz all-optical molecule-plasmon modulation. *Adv. Mater.* **18,** 1645–1648 (2006).
106. Altewisher, E., van Exter, M. P. & Woerdman, J. P. Plasmon-assisted transmission of entangled photons. *Nature* **418,** 304–306 (2002).
107. Fasel, S. *et al.* Energy-time entanglement preservation in plasmon-assisted light transmission. *Phys. Rev. Lett.* **94,** 110501 (2005).
108. Moreno, E., Fernandez-Dominguez, A. I., Cirac, I. J., Garcia-Vidal, F. J. & Martin-Moreno, L. Resonant transmission of cold atoms through subwavelength apertures. *Phys. Rev. Lett.* **95,** 170406 (2005).

Acknowledgements Our research was supported by the European Community, Network of Excellence PLASMO-NANO-DEVICES, STREP SPP, the ANR grant COEXUS, the CNRS, and the French Ministry of Higher Education and Research.

Author Information Reprints and permissions information is available at www.nature.com/reprints. The authors declare no competing financial interests. Correspondence should be addressed to T.W.E. (ebbesen@isis-ulp.org).